Quenching of oscillations via attenuated coupling for dissimilar electrochemical systems

Tanushree Roy ©, J. Escalona ©, and M. Rivera
Centro de Investigación en Ciencias, IICBA, Universidad Autónoma del Estado de Morelos,
Avenida Universidad 1001, Colonia Chamilpa, 62209 Cuernavaca, Morelos, México

Fernando Montoya
Laboratorio de Imágenes y Visión por Computadora, Departamento de Ingeniería Celular y Biocatálisis,
UNAM, 62209 Cuernavaca, Morelos, México

Elizeth Ramírez Álvarez ©
Departamento de Química y Bioquímica, Tecnológico Nacional de México, Instituto Tecnológico de Lázaro Cárdenas,
Avenida Melchor Ocampo 2555, Cuarto Sector, Ciudad Lázaro Cárdenas, 60950 Michoacán, México

Richa Phogat and P. Parmananda
Department of Physics, Indian Institute of Technology, Bombay, Powai, Mumbai 400 076, India

The coupled dynamics of two similar and disparate electrochemical cells oscillators are analyzed. For the similar case, the cells are intentionally operated at different system parameters such that they exhibit distinct oscillatory dynamics ranging from periodic to chaotic. It is observed that when such systems are subjected to an attenuated coupling, implemented bidirectionally, they undergo a mutual quenching of oscillations. The same holds true for the configuration wherein two entirely different electrochemical cells are coupled via bidirectional attenuated coupling. Therefore, the attenuated coupling protocol seems to be universally efficient in achieving oscillation suppression in coupled oscillators (similar or heterogeneous oscillators). The experimental observations were verified by numerical simulations using appropriate electrodissolution model systems. Our results indicate that quenching of oscillations via attenuated coupling is robust and therefore could be ubiquitous in coupled systems with a large spatial separation prone to transmission losses.

I. INTRODUCTION

Collective behaviors observed in coupled nonlinear oscillators range from the inception of spatiotemporal chaos [1,2], synchronization [3–5], and suppression of oscillations [amplitude death (AD) and oscillation death (OD)] [6]. These phenomena of suppression of oscillations are ubiquitous and have been observed in numerous physical, chemical, and biological systems [7–12]. They were first observed experimentally in organ pipes by Lord Rayleigh in the 19th century [13,14]. This quenching of oscillations can be provoked using different techniques such as time-delayed coupling [7,15–20], conjugated coupling [6,21–23], ill-matched timescales [24], and attenuated coupling [25]. The mutual suppression of oscillations is a double edged sword: advantageous and therefore desirable in certain situations, or detrimental, hence avoidable, in other situations [12,26–30]. Among all the above works, Refs. [7,12] stand out as seminal contributions that have inspired our control strategy. In a previous work, the suppression of oscillations using attenuated coupling was achieved for similar oscillators exhibiting autonomous periodic and aperiodic dynamics [25].

In the present paper, we extend this attenuated control protocol to dissimilar systems in an effort to test the ro-bustness of this technique. For this purpose, two entirely different electrochemical cells were configured and coupled. Analogously, two entirely distinct model systems simulating the dynamics of electrochemical corrosion were subjected to attenuated coupling. The paper is organized as follows: In the following section we describe in detail the experimental electrochemical cell device (iron/sulfuric acid) [31–33] and the corresponding evolution equations for a corrosion model [34,35]. In Sec. III, an entirely different electrochemical setup (copper/acetic acid) [36,37] is described in conjunction with an appropriate numerical model [38,39]. In Sec. IV we present both experimental and numerical results observed for different combinations of the two systems. Finally, a brief conclusion in conjunction with the possible applications of this work are presented in Sec. V.

II. SYSTEM 1

A. Experimental setup 1

This electrochemical cell consists of three electrodes. In this case the anode is an iron disk (Alfa Aesar, 6.3 mm diameter, 99.99% purity) shrouded by epoxy, the cathode is a graphite rod (6.15 mm diameter), and the reference is a saturated calomel electrode. This was designed to ensure that
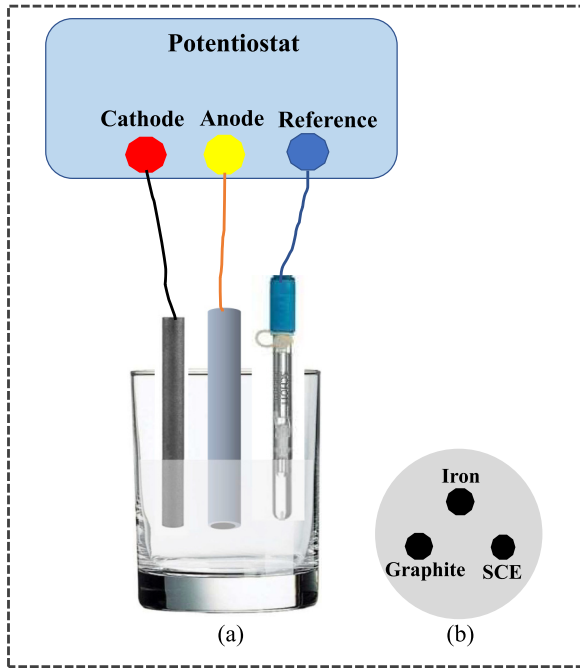
FIG. 1. The schematic of the experimental setup of system 1: (a) The three-electrode electrochemical cell consists of iron (purity 99.99%, diameter 6.3 mm) as the anode, a graphite rod (diameter 6.15 mm) as the cathode, and a saturated calomel electrode as the reference. (b) The cross-sectional view shows the placement of the electrodes.

the anodic reactions (electrodissolution) were restricted to the surface of the anode exposed to the electrolytic solution. The electrolyte solution was a mixture of $1.0M$ sulfuric acid, $0.4M$ potassium sulfate, and a specific concentration of potassium chloride, selected depending on the desired dynamics (chaotic or periodic). A volume of approximately 100 ml was maintained in the cell at room temperature. The schematic of this experimental setup is presented in Fig. 1. In the case of potentiostatic experiments, the anodic voltage $V(0)$ between the anode and the reference electrode is maintained constant. This anodic voltage acts as the control parameter for the system dynamics. Consequently, the current I between the anode and the cathode (anodic current) is the system observable that normally changes its dynamical properties. More details regarding this experimental system are provided in previous works [31–33].

B. Numerical model 1

The first-order differential equations of the Koper-Gaspard model are given in a dimensionless form [34,35],

$$\dot{e} = \frac{v - e}{r} - mk(e)u, \tag{1}$$

$$\dot{u} = -1.25d^{1/2}k(e)u + 2d(w - u), \tag{2}$$

$$\dot{w} = 1.6d(2 - 3w + u), \tag{3}$$

where v is the applied (circuit) potential, e is the "true" electrode potential appearing across the interfacial double layer, r is an adjustable series resistance, d is the transfer rate,

and $k(e)$ is the heterogeneous rate constant determining the rate of electron transfer. To account for the mass transport from the solution to the anode a simple two-diffusion-layer model is applied. Variables u and w are the normalized concentrations of the electroactive species, respectively, in the so-called "surface" and "diffusion" layers, while m is the concentration in the bulk. Equations (1)–(3) are studied under potentiostatic conditions with circuit potential v as the control parameter. For monitoring the behavior we use the total current $i = (v - e)/r$ which is an easily measurable function of the system variables. Since the model equations are not stiff, a simple fourth-order Runge-Kutta method has been applied for integration. The potential-dependent rate constant $k(e)$ is given by a prototype function,

$$k(e) = k_1\theta^2 + k_2 \exp[n\alpha(e - e^0)], \tag{4}$$

where e^0 is the dimensionless standard potential, $n\alpha$ is the transfer coefficient, and θ is related to the surface coverage by some electroactive species. The value of θ is approximated by a sigmoidal function,

$$\theta = \begin{cases} 1 & \text{for } e \leqslant e_d, \\ \exp[-b(e - e_d)^2] & \text{for } e > e_d. \end{cases} \tag{5}$$

Equations (4) and (5) give rise to a potentially unstable electrochemical flux. The extended dynamics of this model, including bifurcation diagrams, can be found in previously published works [34,35]. It needs to be pointed out that there exist an established model [40] for the electrodissolution of iron in sulfuric acid. However, in the present experimental configuration, an additional component has been added (potassium chloride) in order to introduce chaotic behavior. Since this established model is two dimensional (2D), it is unable to capture the dynamics of the modified electrochemical cell, showing chaotic behavior. Therefore, the above Koper-Gaspard model, with similar underlined electrodissolution mechanisms, was chosen since it has three degrees of freedom and is capable of exhibiting both periodic and chaotic dynamics.

III. SYSTEM 2

A. Experimental setup 2

The electrochemical cell was a PAR model K0066/K0060 (Princeton Applied Research). The electrodes were a 0.20-cm^2 copper rotating disk used as the anode, a model K0077 saturated calomel reference electrode (SCE), and a 2.88-cm^2 platinum foil used as a cathode electrode. The copper was obtained in the form of a rod (6 mm diameter, 99.99% purity) from Sputtering Targets Manufacturer. The acetate buffer supporting electrolyte solution was prepared from 30 ml of $2M$ sodium acetate and 70 ml of glacial acetic acid (purity $\geqslant 99.7\%$). Ambient solution temperatures were used. The copper electrode pretreatment consisted of wet sandings down to a grit size of 1000 (2–4 µm). The PAR model 616 rotating disk electrode unit was connected with the PINE AFRDE-5 bipotentiostat. The periodic and chaotic oscillatory data were collected using the appropriate digital to analog converter (DAC) interface platform. More details regarding this experimental system are provided in previous
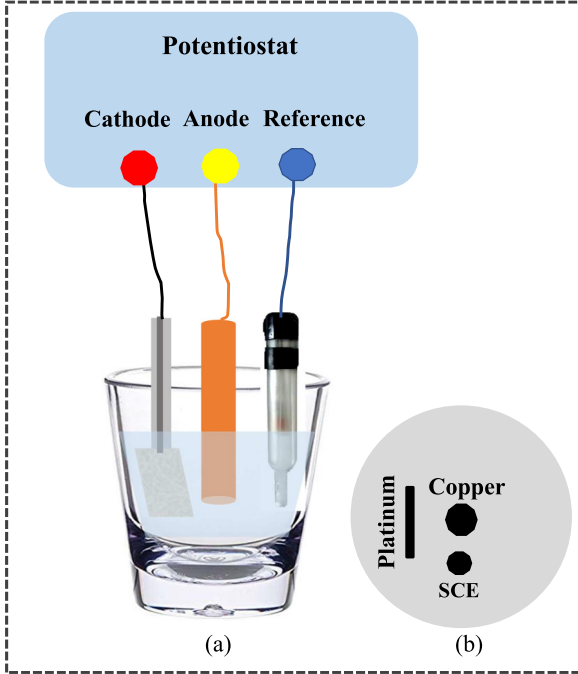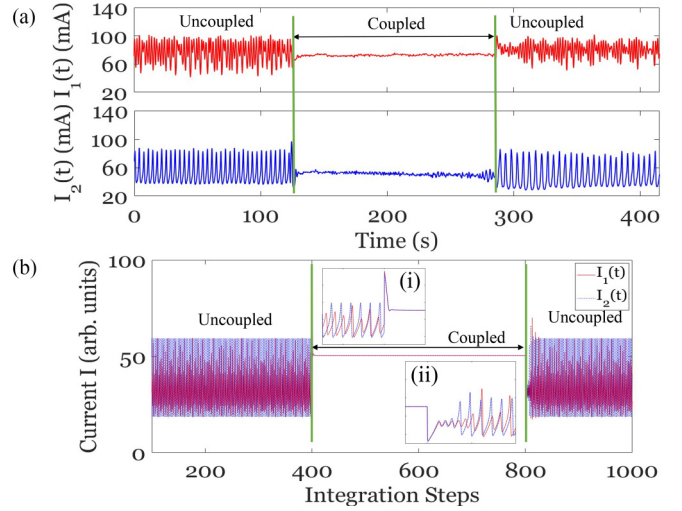
FIG. 3. Quenching of oscillations via coupling of two system 1's exhibiting different autonomous dynamics. (a) Experiments: Dynamics of two coupled electrochemical cells follow the sequence of nncoupled (2 min)→coupled with attenuation (3 min)→uncoupled (∼2 min). The coupling strength was $\gamma = 0.28$ and the attenuation factor was $\alpha = 0.2$. The autonomous chaotic behavior was provoked by maintaining an anodic potential of $V_1(0) = 390$ mV (top panel) and by adding 80 mM potassium chloride in the solution. The autonomous periodic behavior was provoked by maintaining an anodic potential of $V_2(0) = 360$ mV (lower panel) and by adding 40 mM potassium chloride in the solution. (b) Numerics: Corresponding sequence for two coupled model equations. The parameters which are constant for both the oscillators are $r = 0.02$, $m = 120$, $d = 0.11915$, $k_1 = 2.5$, $k_2 = 0.01$, $n\alpha = 0.5$, $e^0 = 30$, $e_d = 35$, and $b = 0.5$. The autonomous chaotic behavior (red) was provoked by $v_1 = 36.74$ and the autonomous periodic behavior was provoked by $v_2 = 36.725$. The coupling strength was $\gamma = 2.0$ and the attenuation factor was $\alpha = 0.8$. In (b), insets (i) and (ii) are the zoomed version of the areas corresponding to 385–410 and 795–820 integration steps, respectively.

FIG. 2. The schematic of the experimental setup of system 2: (a) The three-electrode electrochemical cell consists of copper (purity 99.99%, diameter 6 mm) as the anode, platinum sheet (area of 1.8×1.6 cm^2) as the cathode, and a saturated calomel electrode as the reference. (b) The cross-sectional view shows the placement of the electrodes.

works [36,37]. The schematic of this experimental setup is presented in Fig. 2.

B. Numerical model 2

The numerical model [38,39] is a kinetic rate equation model for metal passivation. The electrochemical system under consideration is the passivation of the reactive surface of a metal electrode in an electrochemical cell. The chemical kinetics of the passivation model includes the formation of two surface films, MOH and MO, where M represents the metal atom. It combines elements from surface reaction models by Talbot and Oriani [39] for MOH and by Sato [41] for MO formation. The chemical kinetics lead to the following dimensionless equations.

$$\dot{Y} = p(1 - \theta_{\text{OH}} - \theta_{\text{O}}) - qY, \qquad (6)$$

$$\dot{\theta}_{\text{OH}} = Y(1 - \theta_{\text{OH}} - \theta_{\text{O}}) - (\exp^{-\beta\theta_{\text{OH}}} + r)\theta_{\text{OH}} + 2s\theta_{\text{O}}(1 - \theta_{\text{OH}} - \theta_{\text{O}}), \qquad (7)$$

$$\dot{\theta}_{\text{O}} = r\theta_{\text{OH}} - s\theta_{\text{O}}(1 - \theta_{\text{OH}} - \theta_{\text{O}}), \qquad (8)$$

where Y is the concentration of metal ions in the electrolyte, θ_{OH} and θ_{O} are the respective fraction of the metal surface covered by each film, p, q, r, and s are parameters related to chemical rate constants, and β represents the non-Langmuir nature of MOH film formation in the Talbot-Oriani model [38,39]. A standard fourth-order Runge-Kutta algorithm was used to integrate the model equations.

IV. RESULTS

A. System 1-system 1

Two electrochemical cells involving the electrodissolution of iron in sulfuric acid buffer were considered. Furthermore, numerics involving two Cu-phosphoric acid models are analyzed. The two experimental cells were mutually coupled under the coupling scheme $V_{1,2} = V_{1,2}(0) + \gamma(\alpha I_{2,1} - I_{1,2})$. In this coupling term $V(0)$ is the corresponding rest potential of each cell, I corresponds to the observable anodic current, γ is the coupling strength, and α is the attenuation factor. The parameter α was tuned precisely to observe the complete dead state (as shown in Fig. 3).

Analogously, the coupling term introduced in the numerical model in Eq. (1) can be written as $\gamma(\alpha e_{2,1} - e_{1,2})$, where γ and α were defined previously and e is one of the model variables. Figure 3 shows both experimental and simulation results indicating quenching of oscillations for the appropriate set of coupling parameters provided in the figure caption. The autonomous dynamics considered here are chaotic and period 1, respectively.
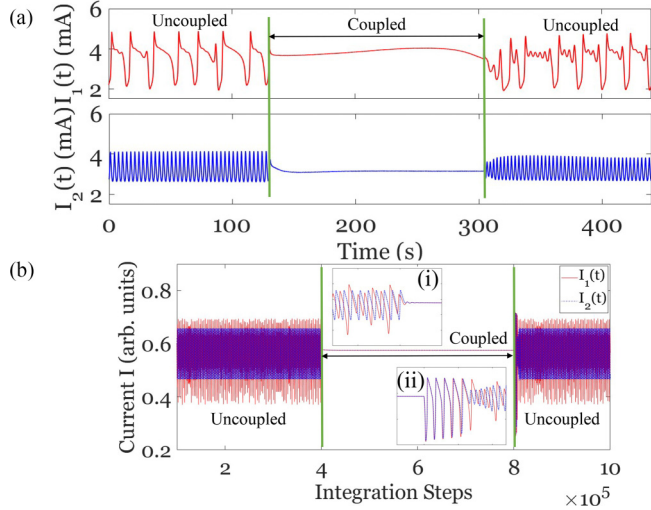
FIG. 4. Quenching of oscillations via coupling of two system 2's exhibiting different autonomous dynamics. (a) Experiments: Dynamics of two coupled electrochemical cells follow the sequence of uncoupled (2 min)→coupled with attenuation (3 min)→uncoupled (∼2 min). The coupling strength was $\gamma = 0.06$ and the attenuation factor was $\alpha = 0.5$. The autonomous chaotic behavior was provoked by maintaining an anodic potential of $V_1(0) = 800$ mV at a rotation rate of 1300 rpm (top panel). The autonomous periodic behavior was provoked by maintaining an anodic potential of $V_2(0) = 820$ mV (lower panel) at a rotation rate of 1000 rpm. (b) Numerics: Corresponding sequence for two coupled model equations. The parameters which are constant for both the oscillators are $p = 2 \times 10^{-4}$, $q = 1 \times 10^{-3}$, $r = 2 \times 10^{-5}$, and $\beta = 5$. The autonomous chaotic behavior (red) was provoked by $s_1 = 9.7 \times 10^{-5}$ and the autonomous periodic behavior (blue) was provoked by $s_2 = 9.63 \times 10^{-5}$. The coupling strength was $\gamma = 0.01$ and the attenuation factor was $\alpha = 0.8$. In (b), insets (i) and (ii) are the zoomed version of the areas corresponding to $(3.92–4.05) \times 10^5$ and $(7.96–8.12) \times 10^5$ integration steps, respectively.

B. System 2-system 2

Two electrochemical cells involving the electrodissolution of copper in acetic acid buffer were considered. Furthermore, numerics involving two units of the model system for the electrodissolution of a metal surface in an aqueous media are analyzed. The two experimental cells were mutually coupled under the coupling scheme $V_{1,2} = V_{1,2}(0) + \gamma(\alpha I_{2,1} - I_{1,2})$. In this coupling term $V(0)$ is the corresponding rest potential of each cell, I corresponds to the observable anodic current, γ is the coupling strength, and α the attenuation factor. Analogously, the coupling term introduced in the numerical model in Eq. (6) can be written as $\gamma(\alpha \theta_{OH_{2,1}} - \theta_{OH_{1,2}})$, where γ and α were defined previously and θ_{OH} is one of the model variables. Figure 4 shows both experimental and simulation results indicating quenching of oscillations for the appropriate set of coupling parameters provided in the figure caption. The autonomous dynamics considered here are chaotic and period 1, respectively. The attenuation factor α was chosen carefully to observe the quenching of oscillations.

C. System 1-system 2

Finally, the ultimate test for the performance of this quenching method was conducted. For this purpose two en-
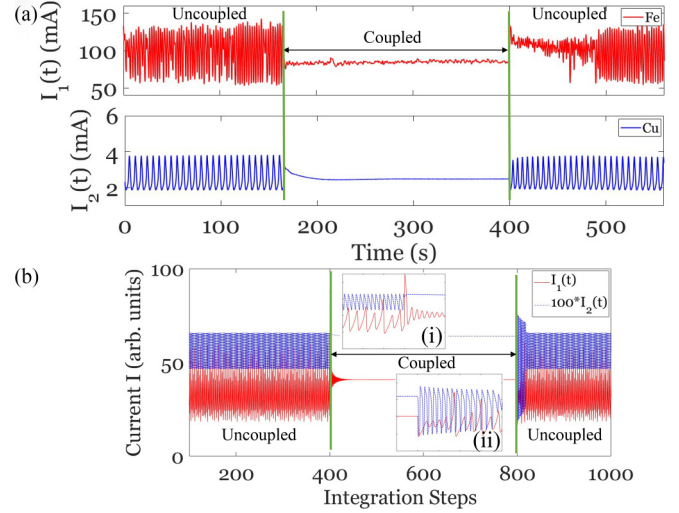

FIG. 5. Quenching of oscillations via coupling of system 1 and system 2 exhibiting different autonomous dynamics. (a) Experiments: Dynamics of two coupled electrochemical cells follow the sequence of uncoupled (2 min)→coupled with attenuation (3 min)→uncoupled (∼2 min). The coupling strength was $\gamma = 0.20$, the attenuation factor was $\alpha = 0.3$, and the amplitude rescaling factor was $\delta = 0.35$. The autonomous chaotic behavior (red) of system 1 was provoked by maintaining an anodic potential of $V_1(0) = 580$ mV (top panel) and by adding 74 mM potassium chloride in the solution. The autonomous periodic behavior of system 2 was provoked by maintaining an anodic potential of $V_2(0) = 850$ mV (lower panel) at a rotation rate of 1200 rpm. (b) Numerics: Corresponding sequence for two coupled model equations. The autonomous chaotic behavior (red) of system 1 was provoked by a set of parameters: $r_1 = 0.02$, $m = 120$, $d = 0.11915$, $k_1 = 2.5$, $k_2 = 0.01$, $n\alpha = 0.5$, $e^0 = 30$, $e_d = 35$, $b = 0.5$, and $v = 36.74$. The autonomous periodic behavior (blue) of system 2 was provoked by a set of parameters: $p = 2 \times 10^{-4}$, $q = 1 \times 10^{-3}$, $r = 2 \times 10^{-5}$, $\beta = 5$, and $s = 9.63 \times 10^{-5}$. The coupling strength was $\gamma = 0.20$, the attenuation factor was $\alpha = 0.1$, the amplitude scaling factor was $\delta = 250$, and the frequency scaling factor was $\tau = 1000$. In (b), insets (i) and (ii) are the zoomed version of the areas corresponding to 385–410 and 795–820 integration steps, respectively.

tirely different electrochemical cells were considered. These cells not only have dissimilar anodes (copper and iron), but also the electrolytic solutions (acetic acid buffer and sulfuric acid) are different. Consequently, the autonomous dynamics of anodic current had dramatically different amplitudes and frequencies. Therefore, appropriate scaling amplitude (δ) and frequency (τ) had to be included when required. To reiterate, two electrochemical cells involving the electrodissolution of iron/sulfuric acid and copper/acetic acid were coupled. These cells were mutually coupled under the coupling scheme: $V_1 = V_1(0) + \gamma(\alpha I_2 - \delta^{-1} I_1)$ and $V_2 = V_2(0) + \gamma(\alpha I_1 - \delta I_2)$. In these equations $[V_1(0), I_1]$ and $[V_2(0), I_2]$ are the rest potentials and anodic currents of iron and copper cells, respectively. The parameter γ is the coupling strength, α the attenuation factor, and δ the amplitude scaling. In this case no frequency scaling was necessary ($\tau = 1$).

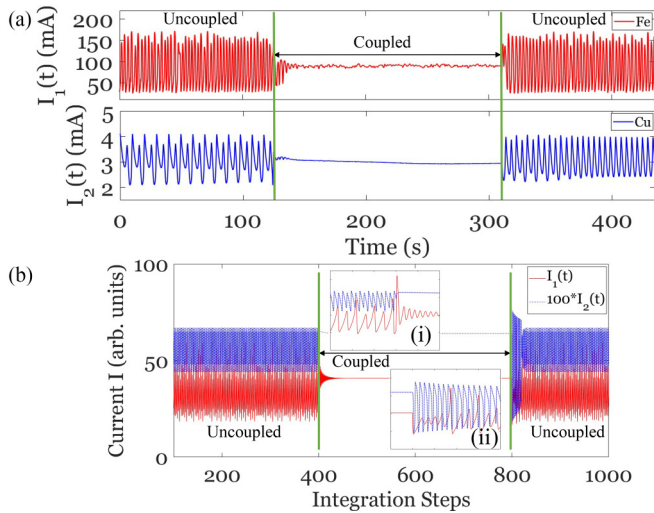Analogously, the coupling terms introduced in the numerical models in Eqs. (1) and (6) can be written as

FIG. 6. Quenching of oscillations via coupling of system 1 and system 2 exhibiting different autonomous dynamics. (a) Experiments: Dynamics of two coupled electrochemical cells follow the sequence of uncoupled (2 min)→coupled with attenuation (3 min)→uncoupled (~2 min). The coupling strength was $\gamma = 0.14$, the attenuation factor was $\alpha = 0.3$, and the amplitude rescaling factor was $\delta = 0.35$. The autonomous chaotic behavior (red) of system 1 was provoked by maintaining an anodic potential of $V_1(0) = 480$ mV (top panel) and by adding 74 mM potassium chloride in the solution. The autonomous period-2 behavior of system 2 was provoked by maintaining an anodic potential of $V_2(0) = 800$ mV (lower panel) at a rotation rate of 1100 rpm. (b) Numerics: Corresponding sequence for two coupled model equations. The autonomous chaotic behavior (red) of system 1 was provoked by a set of parameters: $r_1 = 0.02$, $m = 120$, $d = 0.11915$, $k_1 = 2.5$, $k_2 = 0.01$, $n\alpha = 0.5$, $e^0 = 30$, $e_d = 35$, $b = 0.5$, and $v = 36.74$. The autonomous period-2 behavior (blue) of system 2 was provoked by a set of parameters: $p = 2 \times 10^{-4}$, $q = 1 \times 10^{-3}$, $r = 2 \times 10^{-5}$, $\beta = 5$, and $s = 9.66 \times 10^{-5}$. The coupling strength was $\gamma = 0.20$, the attenuation factor was $\alpha = 0.1$, the amplitude scaling factor was $\delta = 250$, and the frequency scaling factor was $\tau = 1000$. In (b), insets (i) and (ii) are the zoomed version of the areas corresponding to 385–410 and 795–820 integration steps, respectively.
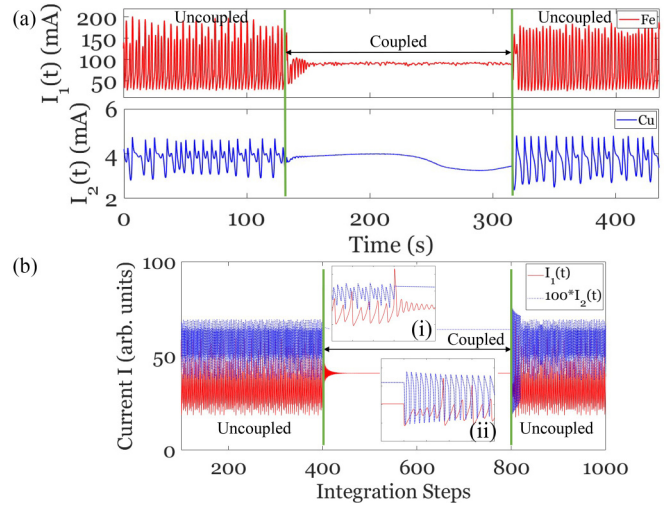
FIG. 7. Quenching of oscillations via coupling of system 1 and system 2 exhibiting different autonomous dynamics. (a) Experiments: Dynamics of two coupled electrochemical cells follow the sequence of uncoupled (2 min)→coupled with attenuation (3 min)→uncoupled (~2 min). The coupling strength was $\gamma = 0.14$, the attenuation factor was $\alpha = 0.2$, and the amplitude rescaling factor was $\delta = 0.35$. The autonomous chaotic behavior (red) of system 1 was provoked by maintaining an anodic potential of $V_1(0) = 500$ mV (top panel) and by adding 74 mM potassium chloride in the solution. The autonomous periodic behavior of system 2 was provoked by maintaining an anodic potential of $V_2(0) = 840$ mV (lower panel) at a rotation rate of 1600 rpm. (b) Numerics: Corresponding sequence for two coupled model equations. The autonomous chaotic behavior (red) of system 1 was provoked by a set of parameters: $r_1 = 0.02$, $m = 120$, $d = 0.11915$, $k_1 = 2.5$, $k_2 = 0.01$, $n\alpha = 0.5$, $e^0 = 30$, $e_d = 35$, $b = 0.5$, and $v = 36.74$. The autonomous periodic behavior (blue) of system 2 was provoked by a set of parameters: $p = 2 \times 10^{-4}$, $q = 1 \times 10^{-3}$, $r = 2 \times 10^{-5}$, $\beta = 5$, and $s = 9.70 \times 10^{-5}$. The coupling strength was $\gamma = 0.20$, the attenuation factor was $\alpha = 0.1$, the amplitude scaling factor was $\delta = 250$, and the frequency scaling factor was $\tau = 1000$. In (b), insets (i) and (ii) are the zoomed version of the areas corresponding to 385–410 and 795–820 integration steps, respectively.

$\gamma(\alpha\delta^{-1}e - Y)$ and $\gamma(\alpha\delta Y - e)$, where γ, α, and δ were defined previously and Y and e are the chosen model variables. Furthermore, all the three evolution equations of system 2 [Eqs. (6)–(8)] were multiplied by τ, the frequency scaling parameter.

Figures 5–7 show three sets of experimental and simulations results indicating quenching of oscillations for dissimilar systems at different combinations of chaotic/periodic dynamics, for the appropriate sets of coupling parameters provided in the figure captions. In Fig. 5(a), α is chosen as 0.3 to observe the quenching of oscillations. For the α value to be higher than 0.3, both oscillators do not exhibit complete dead state when the coupling is on. Therefore, in each configuration, at fixed values of other parameters, only the attenuation factor α was monitored to observe the quenching of oscillations from both the oscillators.

V. SUMMARY AND DISCUSSION

In this paper, we report the quenching of oscillations in two bidirectionally coupled electrochemical cells when their individual signals were attenuated before passing on to the other oscillator. These results seem to be robust for the similar cells (system 1-system 1, system 2-system 2) exhibiting different dynamical behaviors as well as dissimilar (system 1-system 2) cells. This attenuation presented before feeding the signal to the other oscillator is used to mimic a physical situation wherein there is an attenuation of signal amplitude due to various transmission losses. Interestingly, a cessation of oscillations was observed when the signal attenuation crosses a threshold. These experimental observations were reproduced in corresponding numerical models.

These results are a considerable extension upon our previous work wherein a mutual suppression of oscillations was observed for similar systems exhibiting qualitatively identical dynamics. This renders the phenomena of quenching of

oscillations, in the presence of attenuated coupling, almost universal. Our results are relevant to the scenario of coupled systems, regardless of whether the individual units are similar or dissimilar, as long as they have significant spatial separation and hence are liable to a loss of signal strength during the information transmission. For example, neuronal cells, of the same or different genre, coupled over a large distance may suffer from signal attenuation at the receiver's end. Therefore, attenuation-induced oscillation suppression suggests an alternate mechanism for control of oscillatory behavior in neuronal systems [42,43]. Such attenuation of signals also underpins models of distance-dependent coupling that is believed to be widespread in ecological systems [44].

To summarize, attenuated coupling, under appropriate implementation conditions, could lead to the spontaneous stabilization of steady states and offers a potent, almost universal technique for oscillation quenching in coupled nonlinear oscillators.

[1] P. Parmananda and J. L. Hudson, Phys. Rev. E **64**, 037201 (2001).

[2] K. Kaneko, Chaos **2**, 279 (1992).

[3] D. K. Verma, A. Q. Contractor, and P. Parmananda, J. Phys. Chem. A **117**, 267 (2013).

[4] P. Kumar, D. K. Verma, P. Parmananda, and S. Boccaletti, Phys. Rev. E **91**, 062909 (2015).

[5] B. K. Bera, D. Ghosh, P. Parmananda, G. V. Osipov, and S. K. Dana, Chaos **27**, 073108 (2017).

[6] M. Dasgupta, M. Rivera, and P. Parmananda, Chaos **20**, 023126 (2010).

[7] T. Banerjee and D. Biswas, Chaos **23**, 043101 (2013).

[8] B. K. Bera, C. Hens, and D. Ghosh, Phys. Lett. A **380**, 2366 (2016).

[9] T. Biwa, S. Tozuka, and T. Yazaki, Phys. Rev. Appl. **3**, 034006 (2015).

[10] K. Konishi, Phys. Rev. E **68**, 067202 (2003).

[11] Y. Zhai, I. Z. Kiss, and J. L. Hudson, Phys. Rev. E **69**, 026208 (2004).

[12] W. Zou, D. V. Senthilkumar, M. Zhan, and J. Kurths, Phys. Rep. **931**, 1 (2021).

[13] J. Rayleigh, Philos. Mag. **13**, 340 (1882).

[14] A. Pikovsky, M. Rosenblum, and J. Kurths, *Synchronization: A Universal Concept in Nonlinear Sciences* (Cambridge University Press, Cambridge, UK, 2003).

[15] R. Phogat, I. Tiwari, P. Kumar, M. Rivera, and P. Parmananda, Eur. Phys. J. B **91**, 111 (2018).

[16] Y. N. Kyrychko, K. B. Blyuss, and E. Schöll, Eur. Phys. J. B **84**, 307 (2011).

[17] N. Punetha, R. Karnatak, A. Prasad, J. Kurths, and R. Ramaswamy, Phys. Rev. E **85**, 046204 (2012).

[18] F. M. Atay, Phys. Rev. Lett. **91**, 094101 (2003).

[19] A. Sharma and M. D. Shrimali, Phys. Rev. E **85**, 057204 (2012).

[20] A. Sharma, P. R. Sharma, and M. D. Shrimali, Phys. Lett. A **376**, 1562 (2012).

[21] A. Prasad, Phys. Rev. E **72**, 056204 (2005).

[22] R. Karnatak, R. Ramaswamy, and A. Prasad, Phys. Rev. E **76**, 035201(R) (2007).

[23] T. Mandal, T. Singla, M. Rivera, and P. Parmananda, Chaos **23**, 013130 (2013).

[24] S. S. Chaurasia, A. Biswas, P. Parmananda, and S. Sinha, Chaos **31**, 103104 (2021).

[25] I. Tiwari, R. Phogat, A. Biswas, P. Parmananda, and S. Sinha, Phys. Rev. E **105**, L032201 (2022).

[26] D. V. Ramana Reddy, A. Sen, and G. L. Johnston, Phys. Rev. Lett. **85**, 3381 (2000).

[27] I. Ozden, S. Venkataramani, M. A. Long, B. W. Connors, and A. V. Nurmikko, Phys. Rev. Lett. **93**, 158102 (2004).

[28] K. Suresh, M. D. Shrimali, A. Prasad, and K. Thamilmaran, Phys. Lett. A **378**, 2845 (2014).

[29] V. Resmi, G. Ambika, and R. E. Amritkar, Phys. Rev. E **84**, 046212 (2011).

[30] R. Herrero, M. Figueras, J. Rius, F. Pi, and G. Orriols, Phys. Rev. Lett. **84**, 5312 (2000).

[31] J. M. Cruz, M. Rivera, and P. Parmananda, Phys. Rev. E **75**, 035201(R) (2007).

[32] J. M. Cruz, M. Rivera, and P. Parmananda, J. Phys. Chem. A **113**, 9051 (2009).

[33] J. M. Cruz, A. Hernandez-Gomez, and P. Parmananda, Phys. Rev. E **75**, 055202(R) (2007).

[34] M. T. M. Koper and P. Gaspard, J. Chem. Phys. **96**, 7797 (1992).

[35] I. Z. Kiss, V. Gáspár, L. Nyikos, and P. Parmananda, J. Phys. Chem. A **101**, 8668 (1997).

[36] H. D. Dewald, P. Parmananda, and R. W. Rollins, J. Electrochem. Soc. **140**, 1969 (1993).

[37] P. Parmananda, P. Sherard, and R. W. Rollins, Phys. Rev. E **47**, R3003 (1993).

[38] McCoy J. Kevin, P. Parmananda, R. W. Rollins, and A. J. Markworth, J. Mater. Res. **8**, 1858 (1993).

[39] J. B. Talbot and R. A. Oriani, Electrochim. Acta **30**, 1277 (1985).

[40] A. Karantonis and S. Nakabayashi, Chem. Phys. Lett. **347**, 133 (2001).

[41] N. Sato, in *Passivity of Metals*, edited by R. P. Frankenthal and J. Kruger (The Electrochemical Society, Pennington, NJ, 1978).

[42] S. Sinha and W. L. Ditto, Phys. Rev. E **63**, 056209 (2001).

[43] M. P. K. Jampa, A. R. Sonawane, P. M. Gade, and S. Sinha, Phys. Rev. E **75**, 026215 (2007).

[44] T. Banerjee, P. S. Dutta, A. Zakharova, and E. Schöll, Phys. Rev. E **94**, 032206 (2016).